Reactive and Functional Polymers 206 (2025) 106109

Contents lists available at ScienceDirect

Reactive and Functional Polymers

journal homepage: www.elsevier.com/locate/react

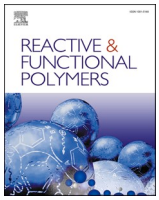

Custom-shaped malleable, recyclable and reversible structural adhesives based on vanillin polyimine vitrimers

Anna Vilanova-Pérez [a], Marc Surós [a,b], Àngels Serra [c], Silvia De la Flor [a,*], Adrià Roig [c,d,**]

[a] Universitat Rovira i Virgili, Department of Mechanical Engineering, Av. Països Catalans 26, 43007 Tarragona, Spain
[b] Eurecat – Chemical Technology Unit, C/ Marcel·lí Domingo 2, 43007 Tarragona, Spain
[c] Universitat Rovira i Virgili, Department of Analytical and Organic Chemistry, C/ Marcel·lí Domingo 1, Edif. N4, 43007 Tarragona, Spain
[d] Ghent University, Department of Organic and Macromolecular Chemistry, Faculty of Sciences, Polymer Chemistry Research group, Krijgslaan 281-S4bis, Ghent 9000, Belgium

ARTICLE INFO

Keywords:
Vanillin
Polyimine
Vitrimer
Recyclability
Malleability
Reversible adhesives

ABSTRACT

A series of polyimine vitrimers were prepared from a synthesized dialdehyde derivative of vanillin. This derivative was then crosslinked with two different ratios of amines (Jeffamine T403 and m-xylylenediamine), forming imine bonds responsible for the exchange reactions. This process resulted in three distinct materials which exhibited glass transition temperatures (T_gs) ranging from 20 to 60 °C, along with good thermal stability, and strong mechanical and thermomechanical properties.

Their dynamicity resulted in a fast relaxation rate achieving a complete relaxation in less than 15 min at 140 °C. Additionally, the polyimines could be mechanically recycled up to three times without significant loss in their final properties, demonstrating the possible enhancement of their lifespan. Moreover, they could be chemically recycled under mild conditions through acid hydrolysis or transamination, which significantly contributes towards a better circular economy. Furthermore, these vitrimers were tested as reversible structural adhesives, achieving initial lap-shear strength values of 12.4 MPa and up to 97 % of efficiency after re-bonding, highlighting their huge potential for industrial applications. Due to their pre-cured state, these adhesives were malleable, which allow them to be custom-shaped into different complex shapes. Finally, these imine materials showed outstanding self-welding capabilities with the repaired versions showing comparable performance to the original.

1. Introduction

Thermosetting materials have been used in a wide range of applications due to their great thermal and chemical resistance, as well as outstanding mechanical properties. Some of the most common uses of these materials are in composite or coating industries, which account for more than 15 % of overall plastic consumption [1]. However, over the last century, the development of new polymers specifically tailored for adhesive purposes has been skyrocketing, becoming very attractive in academic and industrial fields [2–5].

While structural adhesives are highly useful and have numerous everyday applications, their non-recyclability is a significant drawback. Once cured, their covalently cross-linked 3D network prevents not only reuse in manufacturing but also repair during service and recovery of the initial adherents [6]. For this reason, the use of covalent adaptable networks (CANs) in the design of adhesives represents a promising solution to overcome this problem. Their ability to flow when certain stimulus is applied, enables the repairability of the adhesive and their possible re-use during the service life [7,8]. Thus, at the end of their lifespan, CANs can be mechanically recycled and, in some cases, chemically recycled, which offers the possibility to recover the adherent in the field of adhesives [9]. Thus, these materials could maintain the properties of conventional structural adhesives at service temperatures but, at the same time, be reprocessed like thermoplastics [10–13]. Organic reactions such as transesterification [14–16], disulfide exchange [17–19] or transamination of vinylogous urethanes [20,21],

* Corresponding author
** Corresponding author at: Universitat Rovira i Virgili, Department of Analytical and Organic Chemistry, C/ Marcel·lí Domingo 1, Edif. N4, 43007 Tarragona, Spain.
E-mail addresses: silvia.delaflor@urv.cat (S. De la Flor), Adria.RoigGibert@UGent.be (A. Roig).

https://doi.org/10.1016/j.reactfunctpolym.2024.106109
Received 3 September 2024; Received in revised form 4 November 2024; Accepted 20 November 2024
Available online 23 November 2024

among others, have been extensively used to design CANs with tunable properties for a wide range of applications. However, the exploitation of these materials as reversible and reusable structural adhesives is still in the early stages, and only few reports can be found in the literature [17,20,22–24].

Imines are one of the most important types of associative CANs, also called vitrimers due to their rapid relaxation rates even without the use of any external catalyst making them excellent for recycling and re-bonding even at low temperatures [23,25]. Moreover, they can be hydrolyzed under mild acidic conditions, which usually offers the possibility to recover the initial monomers, representing a major step towards a better circularity. Therefore, at the end of service life not only the adhesive can be recycled and reprocessed but also the adherent reused and recovered. In addition, the development of imine vitrimers also provides the chance to align with the current tendency of using renewable and bio-based reagents as substituents of petrol-based resources [26,27]. Compounds such as vanillin, syringaldehyde or 2,5-furandicarboxaldehyde, which can be easily obtained from renewable resources such as lignin or carbohydrates, are currently being used to prepare imine-based thermosets with different properties due to their aldehyde group and different functionalities [28–30].

However, in the field of reversible adhesives, imines still have not been deeply studied. In this context, Zhou et al. reported a series of polyimine vitrimers by synthesizing different aldehydes from vanillin, cured with two different commercial bio-based aliphatic amines [23]. All the materials obtained exhibited excellent dynamic and thermal properties, and they could be mechanically reprocessed and recycled back to the starting monomer in a closed-loop fashion. However, only one material showed good lap-shear strength value with an 85 % of efficiency in the re-bonding. More recently, Li et al. used cysteamine-functionalized castor oil and a divanillin derivative to prepare four different fully bio-based polyimine vitrimers [31]. All these materials exhibited T_gs below room temperature and showed good self-healing properties, being able to be recycled up to 3 times. Focusing on the adhesive performance, one material showed 6.1 MPa in lap-shear strength but the re-adhesion or dismantling was not tested.

Taking all this into consideration, in the present work, a series of polyimine vitrimers has been prepared from a synthesized dialdehyde (GV) derived from bio-based vanillin cured with different proportions of Jeffamine T403 (Jeff T403) and *m*-xylylenediamine (mXDA) (Scheme 1).

The thermal and thermomechanical properties of all vitrimers were evaluated and their dynamicity deeply studied through rheological analysis. Mechanical reprocessing was demonstrated, and their chemical recyclability assessed in order to recover the initial monomer in a closed-loop fashion. In addition, thanks to a pre-cured state, custom-shaped malleable adhesives were prepared and tested in lap-shear tests which were also used to evaluate the re-bonding after failure. Finally,

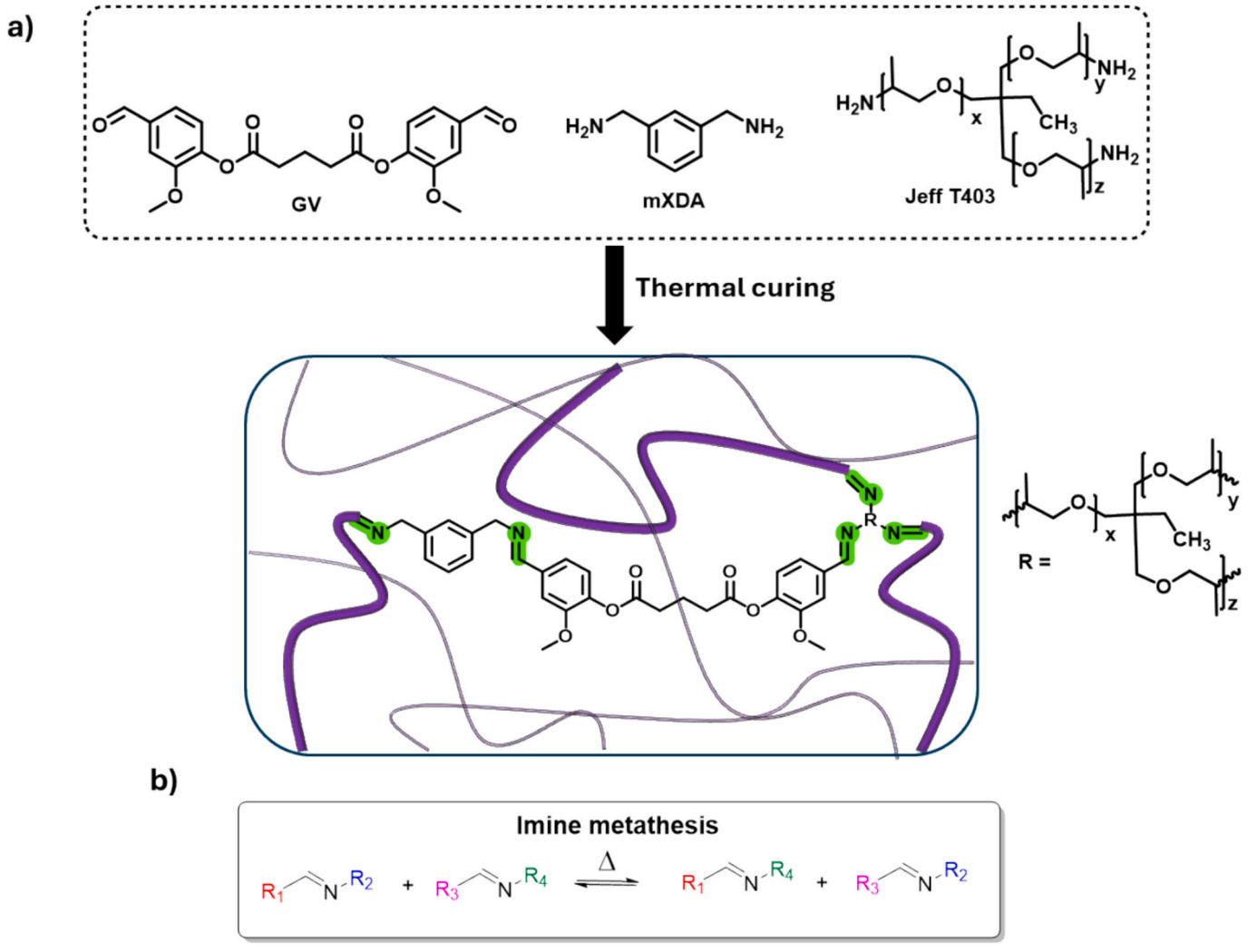

Scheme 1. Chemical structures of the monomer and amines used in the preparation of the materials and chemical structure of polyimines after thermal curing. b) Dynamic imine metathesis exchange.

polyimines also showed good self-welding and repairing properties.

2. Experimental part

2.1. Materials

Trimethylolpropane tris[poly(propylene glycol), amine terminated] ether (Jeffamine T403) was purchased from Sigma Aldrich. m-Xylylenediamine (mXDA) and butylamine were provided by TIC. Ethylenediamine was purchased from Fluorochem. Hydrochloric acid (HCl) was purchased from Fischer Chemical. Glutaryl chloride (GC), vanillin (Van) and magnesium sulfate ($MgSO_4$) were obtained from ThermoFisher Scientific and triethylamine (TEA), sodium hydroxide (granulated, NaOH) and dichloromethane (DCM) were obtained from Scharlau.

2.2. Synthesis of the dialdehyde derivative of vanillin (GV)

Van (18.45 g, 12.12 mmol) was added to a 250 mL three-necked round bottom flask equipped with a magnetic stirrer and purged with argon. Then, 80 mL of dry DCM were added, and the mixture was cooled to 0 °C in an ice bath, followed by the addition of TEA (18.77 g, 18.55 mmol). Finally, a solution of GC (10 g, 59.17 mmol) in 20 mL of dry DCM was added dropwise within 30 min while the mixture was kept at 0 °C. Afterwards, the mixture was kept at room temperature for 24 h. After that, the mixture was vacuum filtered to remove the salt by-product and the obtained liquid was washed with 150 mL of 1 M HCl, 150 mL of water, 150 mL of 1 M NaOH and several times with water. Finally, the organic phase was dried over anhydrous $MgSO_4$, filtered, and concentrated in a rotary evaporator to obtain GV as a white powder (95 % yield). Mp (by DSC): 105 °C. ^{1}H NMR ($CDCl_3$, δ in ppm): 9.92 (s, 1H), 7.51–7.26 (m, 3H), 3.91 (s, 3H), 2.83 (t, 2H), 2.26 (m, 2H) (Fig. S1). ^{13}C NMR ($CDCl_3$, δ in ppm): 191.02, 170.36, 151.93, 144.91, 135.32, 124.80, 123.39, 110.84, 56.07, 32.75, 20.16 (Fig. S2).

2.3. Preparation of polyimine vitrimers

Polyimine vitrimers were prepared by reacting GV with the corresponding amines in molar stoichiometric conditions NH_2/aldehyde 1:1. In the case of vitrimers with mixed proportions of amines, the mols of aldehyde were first calculated, and a certain percentage of them were reacted with NH_2 groups of Jeff T403. The remaining percentage was reacted with NH_2 of mXDA. The preparation consists of first dissolving GV (500 mg) in 4 mL of DCM and then adding the corresponding amount of amine(s). The mixture was poured into a glass Petri plate and kept overnight at room temperature in a fume hood. Then, the pre-cured film was die-cut with the desired shape (Fig. S3) and cured for 6 h at 120 °C and 4 h at 140 °C. The samples were encoded as JX, where X is the molar percentage of aldehydes that react with NH_2 groups from Jeff T403. The remaining molar percentage corresponds to the aldehydes reacting with NH_2 groups of mXDA. For example, J75 refers to a sample in which 75 % of mols of aldehyde have reacted with NH_2 of Jeff T403, and 25 % have reacted with NH_2 of mXDA. The specific composition for each material is summarized in Table 1.

2.4. Characterization techniques

^{1}H NMR and ^{13}C NMR spectra were recorded on a Varian VNMR-S400 NMR spectrometer using $CDCl_3$ as the solvent. All chemical shifts are quoted on the δ scale in part per million (ppm) using the residual protonated solvent as the internal standard (^{1}H NMR: $CDCl_3$ = 7.26 ppm; ^{13}C NMR: $CDCl_3$ = 77.16 ppm).

A Jasco FT/IR-680 Plus spectrometer equipped with an attenuated total reflection accessory (ATR) (Golden Gate, Specac Ltd., Teknokroma) was used to register the FTIR spectra of the synthetized monomer and the cured materials, as well as to characterize the materials after chemical and mechanical recycling. Real-time spectra were registered in the wavenumber range between 4000 and 600 cm^{-1} with a resolution of 4 cm^{-1} averaging over 32 scans.

Differential scanning calorimetry (DSC) analyses were carried out on a Mettler DSC3+ instrument calibrated with indium (heat flow calibration) and zinc (temperature calibration) standards. Cured samples of approximately 8–10 mg were placed into aluminum pans with pierced lids and analyzed under a N_2 atmosphere with a gas flow of 50 $cm^3 \cdot min^{-1}$ at a heating rate of 20 °C·min^{-1} to determine the glass transition temperature (T_g).

The thermal stability of the vitrimers was evaluated using a Mettler Toledo TGA 2 thermo-balance. Cured samples weighing around 10 mg were degraded between 30 and 600 °C at a heating rate of 10 °C min^{-1} under a N_2 atmosphere with a flow rate of 50 $cm^3 \cdot min^{-1}$.

The thermomechanical properties were evaluated using a thermodynamic mechanical analyzer DMTA Q850 (TA Instruments) equipped with a film tension clamp and a cooling systems ACS 3+. Prismatic rectangular samples with dimensions of around 30 × 5 × 1.5 mm^3 were analyzed from −50 °C to 150 °C at 1 Hz, with 0.1 % strain and at a heating rate of 2 °C·min^{-1}.

The same equipment and clamp were used to evaluate the creep behavior at 0 °C (where all the materials are in its glassy state). Samples with the same dimensions as in the previous test were stretched under a stress of 1 MPa for 30 min, then the stress was immediately released, and the sample was left to recover for 60 min.

The stress-relaxation analyses were conducted with a HR-20 rheometer (TA Instruments) equipped with an electrically heated plate device (EHP) and parallel plate geometry. To evaluate the stress relaxation behavior, the samples were firstly equilibrated at the desired temperature for 3 min, and a constant strain of 1 % (within the linear viscoelastic regime (LVR)) was applied for 100 min, measuring the consequent relaxed modulus as a function of time. Stress relaxation tests were conducted at different temperatures using the same plate.

Subsequently, the dynamic behavior of the materials was fitted using the simple Kohlraush-Williams-Watts (KWW) model [32,33] (Eq. 1):

$$\frac{G(t)}{G_0} = exp\left[-\left(\frac{t}{\tau^*}\right)^{\beta} \right] \quad (1)$$

where $G(t)/G_0$ is the normalized modulus at relaxation time t, τ^* is a characteristic relaxation time and β ($0 < \beta \leq 1$) is the exponent that controls the shape of the stretched exponential decay and reflects the breadth of the relaxation, much smaller β value indicating an extremely broad distribution of relaxation times (KWW model) [34]]. With the relaxation times obtained at each temperature (T), the activation energy values (E_a) were calculated by using an Arrhenius-type equation:

$$ln(\tau) = \frac{E_a}{RT} - ln\, A \quad (2)$$

where A is the pre-exponential factor and R is the gas constant.

Tensile and lap-shear tests were conducted at room temperature using an electromechanical universal testing machine (Shimadzu AGS-X) with a 1 kN load cell at 5 mm·min^{-1} to explore the mechanical properties. Dog-bone-shaped samples Type *V* were tested until failure according to ASTM D638–14 standard to determine the stress and strain at break and the tensile modulus of all materials [35]. Lap-shear tests were carried out using aluminum platens 6060 T66 of dimensions 100 × 25 × 2 mm^2, according to UNE-EN ISO 1465:2009 standard [36]. The

Table 1
Nomenclature and composition of all the prepared polyimines vitrimers.

Sample	GV (mg)	GV (mmols)	Jeff T403 (mg)	Jeff T403 (mmols)	mXDA (mg)	mXDA (mmols)
J100	500	1.19	350.5	0.80	–	–
J75	500	1.19	262.9	0.60	40.7	0.30
J50	500	1.19	175.3	0.40	81.4	0.60

aluminum platens surface was prepared according to UNE-EN ISO 13887:2004 standard [37]. Overlapping regions were degreased with acetone and then mechanically abrased with P180 sandpaper and cleaned again with acetone to remove possible impurities. Then, pre-cured material of rectangular shape of around 25 × 12.5 × 0.2 mm^2 were placed in the overlapping region and completely cured following the previous curing procedure applying 3 kPa of constant pressure to ensure a good contact between the adhesive and the adherents. For the re-bonding tests, the aluminum platens were overlapped again without adding new adhesive and kept for 3 h at 130 °C with a constant pressure of 3 kPa for the subsequent lap-shear test. To check the surface of the aluminum plate before and after the lap-shear test, a digital microscope (Leica DMS1000) was used.

2.5. Reprocessability of the polyimine vitrimers

Samples of vitrimers were ground and hot-pressed at 130 °C for 2 h under 5 kPa applied with a manual hydraulic hot press (Specac Atlas 15 T) obtaining thin round samples that were die-cut for their use in specific thermomechanical and mechanical tests.

2.6. Chemical degradability of the vitrimers

The chemical degradability was assessed following two different pathways:

2.6.1. Acid hydrolysis

vitrimers were poured into a beaker and immersed in a 1 M HCl/THF (1:8 *v*/v) solution for 1 h at room temperature. To try to recover the original monomer, the resulting solution was transferred to an extraction funnel with ethyl acetate, washed once with 1 M HCl and brine, dried over $MgSO_4$, filtered and concentrated in a rotary evaporator.

2.6.2. Transamination

the polyimine materials were placed into a round bottom flask and then, n-butylamine or ethylenediamine were added and kept 10 min at room temperature for the former and 2 h at 110 °C for the latter. Afterward, the mixture was concentrated in a rotary evaporator to remove the excess of free amines. Finally, the obtained product was analyzed.

The solvent resistance of all the materials was also evaluate using three solvents with different polarities: H_2O, ethyl acetate and toluene, from more polar to less polar. The samples remained immersed in the solvents for 24 h and pictures were taken to evaluate the solvent resistance.

3. Results and discussion

3.1. Study of the curing process

Polyimine vitrimers were obtained by condensation reaction of the synthesized dialdehyde (GV) derived from vanillin with different proportions of two amines (Jeff T403 and mXDA) which will allow tailoring the properties of the final materials. Three different polyimines were prepared (J100, J75 and J50). The curing process was evaluated by FTIR, as the release of water makes the interpretation by DSC much more difficult. FTIR analyses were conducted on GV and the cured materials to confirm the completion of the curing. Fig. 1 shows the FTIR spectra of GV (grey) and J100 (light blue) where it is possible to see that the characteristic absorbance band of the aldehyde at 1690 cm^{-1} has completely disappeared in the spectrum of the cured material, while the band corresponding to the imine bond at 1650 cm^{-1} has appeared, confirming the completion of the reaction. It is important to highlight that GV contains ester groups susceptible to suffer the attack of free amines to form the corresponding amides. However, in this case, the amines selectively reacted with aldehydes at these conditions since the band at 1760 cm^{-1} corresponding to the ester remained unaltered after the whole curing process. Fig. S4 collects the FTIR spectra of all the polyimine materials, in which it is possible to observe that there are no significant differences between them regardless of the proportions of amines used, indicating also a successful curing for J75 and J50.

The glass transition temperature (T_g) of the final materials was determined by DSC analysis, and the values obtained are presented in Table 2. Despite the higher functionality of Jeff T403, the increase of mXDA content in the material results in higher T_gs due to the high content of aromatic rings which provides higher rigidity in the final materials. Moreover, the DSC thermograms (Fig. S5) showed no residual exothermal peaks after the T_g, which suggests the completion of the curing.

3.2. Thermomechanical and thermogravimetric characterization of the materials

The thermomechanical properties of the three cured materials were analyzed using DMTA analysis. Fig. 2 shows the evolution of tan δ,

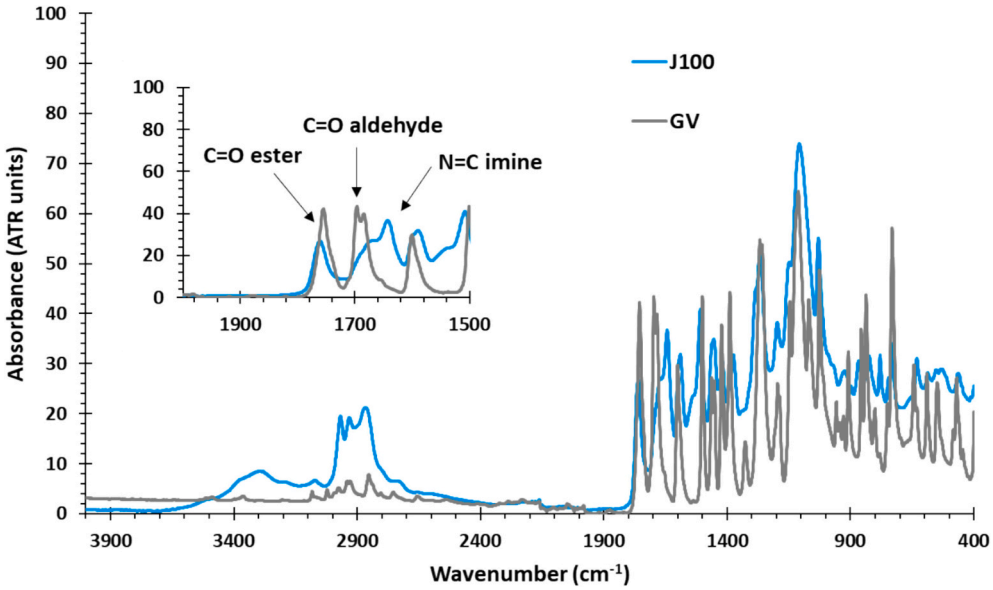

Fig. 1. FTIR spectra of the synthesized dialdehyde GV (grey) and the cured J100 material (light blue).

Table 2
Thermomechanical and thermogravimetric data for the materials prepared.

Sample	T_g [a] (°C)	E'_{glassy} [b] (MPa)	$E'_{rubbery}$ [c] (MPa)	$T_{E''\ loss}$ [d] (°C)	$T_{tan\ \delta}$ [e] (°C)	FWHM [f] (°C)	Cross-link density [g] (mol/m^3)	$T_{2\%}$ [h] (°C)	T_{max} [i] (°C)	Char yield [j] > (%)
J100	31	2497	1.7	18	26	14	195	217	406	7.5
J75	42	2224	1.6	33	44	18	175	215	397	12.5
J50	51	2122	1.4	43	56	21	148	210	391	24.6

[a] T_g obtained by DSC.
[b] Glassy storage modulus at T_g - 50 °C.
[c] Rubbery storage modulus at T_g + 50 °C.
[d] Temperature at the maximum of the peak of loss modulus.
[e] Temperature at the maximum of *tan* δ peak at 1 Hz.
[f] Full width at half maximum of the *tan* δ peak.
[g] Crosslink density calculated with Eq.3.
[h] Temperature of 2 % of weight loss.
[i] Temperature of the maximum rate of degradation.
[j] Char residue at 600 °C.

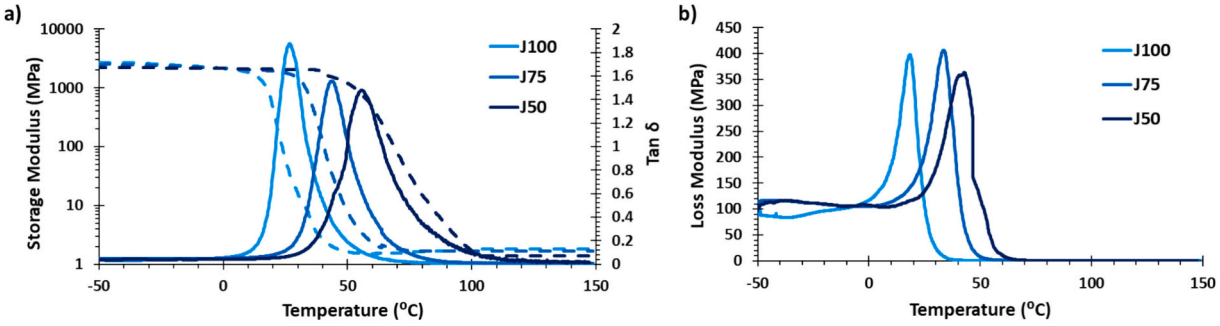

Fig. 2. Evolution of a) storage moduli (*E'*) and tanδ and b) loss moduli (*E''*) with temperature for all the polyimines.

storage (*E'*) (a) and loss (*E''*) (b) moduli with temperature and the most relevant data are summarized in Table 2. As shown in Fig. 2a, the lower the content of the long aliphatic Jeff T403, the higher the $T_{tan\ \delta}$ value (maximum of the peak of the *tan* δ curve) which is in accordance with the DSC analysis. Conversely, a higher amount of Jeff T403 leads to higher rigidity (see values of E'_{glassy}) and higher $E'_{rubbery}$ values, which can be explained by its higher functionality. To confirm this assertion the crosslinking density was calculated by using the relationship presented in Eq.3.

$$d = \frac{E'_{Rubbery}}{3R(T_{tan\delta} + 40)} 10^6 \quad (3)$$

where d is the crosslinking density, $E'_{Rubbery}$ is the storage modulus in the rubbery state (in MPa), R is the gas constant and $T_{tan\ \delta}$ is the temperature of the peak of the tan δ curve. Indeed, the higher functionality of Jeff T403, results in slightly higher crosslinking density which explains the higher $E'_{rubbery}$ value of J100 in comparison to J75 and J50 (see Table 2).

Furthermore, a decrease in the content of Jeff T403 also results in broader *tan* δ peaks (FWHM) due to the higher heterogeneity of the final network. Looking at the evolution of the loss modulus with temperature (Fig. 2b), which represents the viscous part of the amount of energy dissipated during heating, it can be appreciated that in all the cases, the curves follow the same trend as the tan δ curves with no significant differences.

The thermal stability of the materials was studied using thermogravimetric analysis. Fig. 3a and b show the non-isothermal degradation curves and the corresponding derivative curves while the most important data are presented in Table 2. From the curves it can be seen that all the materials follow a similar degradation trend, with a main degradation peak around 400 °C, which can be ascribed to a simultaneous breakage of all bonds. All samples lose 2 % of weight above 210 °C, which suggest that a safe recycling can be performed below this temperature without losing the structural integrity of the materials. As expected, the materials with a higher content of aromatic rings in the

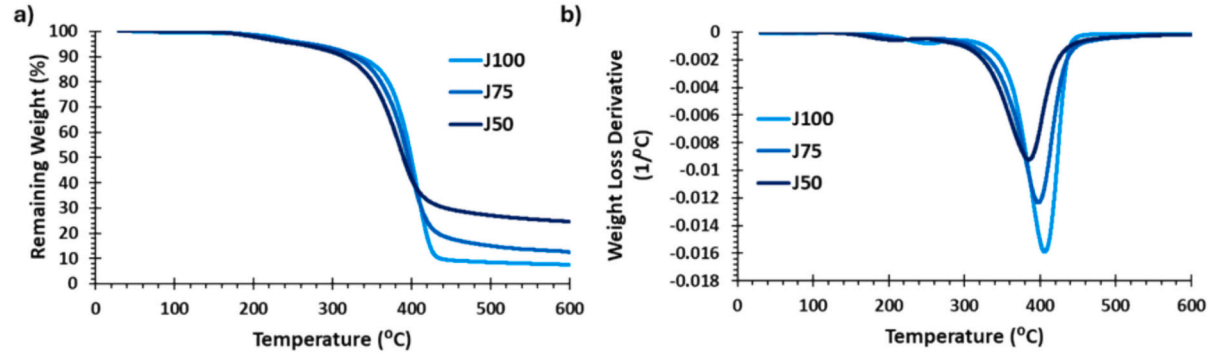

Fig. 3. a) Thermogravimetric curves in N_2 atmosphere and b) DTG curves of all materials.

network exhibit higher values of char yield.

3.3. Mechanical characterization

Tensile stress-strain tests were performed to evaluate the mechanical properties of all the polyimine vitrimers at service temperatures and the effect of the network architecture on those properties. Fig. S6 compares the engineering stress-strain curves at room temperature, and the main data are summarized in Table 3. Stress-strain tests revealed that J100 behaves as an elastomer capable of elongate more than 200 % of its initial length. J75 also behaves as an elastomer, although it can withstand more stress thanks to its rigid aromatic structure. However, its ductility is lower than J100, reaching only 150 % strain at break. Finally, as expected, J50 behaves as a thermoset without any plastic deformation, showing its high brittleness that considerably limits its strength.

It is essential to highlight that, at room temperature, these materials are in between the glassy and the rubbery states (see Fig. 2), therefore, their mechanical properties cannot be entirely compared since they are highly dependent on their T_g. For this reason, DMTA in a static force-controlled mode in tensile was used to evaluate Young's moduli of the vitrimers at temperatures well above and below T_g (± 50 °C) to fully understand how their chemical structure affects their thermomechanical characteristics. As it can be deduced from Table 3, as the aromatic content in the material increases (higher content of mXDA), higher values of E_T are obtained, resulting in more rigid samples at low temperatures or glassy state ($E_{T\ (Tg-50)}$), which additionally, appear to be of the same order of magnitude when compared to E'_{glassy} (see Table 2). However, the opposite trend can be observed at high temperatures where all the materials are in the rubbery state ($E_{T\ (Tg+50)}$). Therefore, their mechanical properties are dependent on the crosslinking density and the lower functionality of mXDA (less crosslinked structures) leads to less rigid materials.

3.4. Study of the vitrimeric behavior of the materials

Stress-relaxation analyses were performed under shear stress using the parallel geometry in the rheometer. After the pre-curing stage to remove DCM, the solid pre-cured films were die-cut in circles of 25 mm diameter and 0.2 mm in thickness, placed between the two plates in the rheometer and further cured before the stress-relaxation analyses. Fig. 4a shows the stress-relaxation curves at different temperatures for J100, while Fig. 4b shows the stress-relaxation curves of all materials at 130 °C for comparison purposes. The relaxation curves of J75 and J50 at all temperatures can be found in Fig. S7. In all the cases the KWW model was used to study the dynamic behavior and the data can be found in Table 4 and Table S1.

As seen in Fig. 4a, J100 polyimine could completely relax the initial stress in a fast way at all temperatures, even at low temperatures such as 110 °C in less than 3000 s (Table S1) without the addition of any external catalyst. However, when J100 is compared to J75 and J50 (Fig. 4b) it can be observed that J75 and J50 need longer times (or higher temperatures) to relax the stress. This can be ascribed to the higher network's mobility provided by the long aliphatic chain of Jeff T403, which makes the exchange reaction between imines more likely to occur, which undoubtedly leads to faster relaxation rates in J100. Reducing the proportion of Jeff T403, results in a higher hindrance of the chains' movement, probably enhanced by the π-π interactions, which make the imine metathesis more difficult to occur.

To further evaluate and understand their vitrimeric behavior, the stretching decay (or KWW) model was used to fit the stress relaxation curves. As can be seen in Table 4 and Table S1, the characteristic relaxation time at 130 °C and β parameter has been calculated for each temperature. By plotting each relaxation time with the inverse of the temperature, an Arrhenius-type correlation can be found (Fig. S8) which allows to calculate the activation energy (E_a) of the exchange process. As it can be observed, the E_a increases with the content of mXDA which indicates a higher sensitivity of the relaxation time with temperature in J50.

Creep tests were performed to analyze and compare the creep behavior of the materials. All the materials were tested at 0 °C, ensuring they were in the glassy state. Fig. S9 presents the creep tests for J100, J75 and J50 materials. As observed, the increase in the strain when the stress is maintained is almost negligible in J75 and J50, while in J100, creep is considerable, as expected. Concerning the recovery process, after 1 h, J50 can recover the strain almost fully, J75 recovers 45 % (compared to the instant strain after unloading) with a slight apparent permanent deformation, and J100 only around 20 % with a considerable plastic (permanent) deformation.

Table 3
Engineering stress and strain at break and tensile modulus of all the polyimine materials.

Sample	σ_b[a] (MPa)	ε_b[b] (%)	$E_{T\ (Troom)}$[c] (MPa)	$E_{T\ (Tg-50)}$[d] (MPa)	$E_{T\ (Tg+50)}$[e] (MPa)
J100	20 ± 1	208 ± 25	399 ± 10	1801 ± 64	2.8 ± 0.1
J75	35 ± 2	137 ± 11	878 ± 15	1903 ± 81	2.5 ± 0.1
J50	25 ± 2	5 ± 2	995 ± 15	2062 ± 84	1.4 ± 0.1

[a] Stress at break.
[b] Strain at break.
[c] Tensile modulus at T_{room}.
[d] Tensile modulus at T_g - 50 °C.
[e] Tensile modulus at T_g + 50 °C.

3.5. Analysis of the adhesion and re-bonding properties

Lap-shear tests were performed to evaluate the adhesion properties of the materials at room temperature. As explained in the Experimental Section, the curing process of these materials first involves a pre-curing state in which the DCM is evaporated after some hours, which results in a gelled and highly malleable pre-cured material. Thanks to that, the adhesive can be die-cut with the specific requirements of the joint and adapt the adhesive layer to complex adhesion surfaces, making possible to obtain complex-shaped joints, which highlights the huge potential of these polyimines for the adhesive manufacturing industry (see Fig. S3). Thus, the pre-cured films were die-cut to the required UNE standard rectangular shapes, placed between the two pretreated surface aluminum plates and cured in a conventional oven while applying 3 kPa to ensure an optimal contact. Fig. 5 shows the lap-shear curves resulting from the tests, and Table 5 presents the main extracted data.

As can be seen, polyimine vitrimeric adhesives showed lap-shear strength values ranging from 3.8 MPa for J50 to 12.4 MPa for J100, which are similar or even higher than previously reported vitrimeric adhesives with similar thermomechanical characteristics [23,31,38]. This difference between adhesives can be explained through the network architecture of the materials as well as their dynamic behavior. The higher the content in Jeff T403, the higher mobility and flexibility, which leads to a less gelled and more malleable pre-cured material that can facilitate adhesion. Moreover, this flexibility facilitates the flow at high temperatures which undoubtedly enhance the adhesion in J100. On the contrary, the lower the content on Jeff T403, the higher the brittleness of the material, which leads to low adhesive strength (see J50). These results are in accordance with the mechanical properties of the materials. However, all the materials yield adhesive-type failures (Fig. S10), which can probably be improved by using another surface treatment that better fits this chemistry. For this reason, further upcoming studies will be focused on the enhancement of the surface treatment.

Thanks to the excellent dynamic behavior of these materials, we envisioned the possible re-adhesion after failure. Thus, the two aluminum plates obtained after the first lap-shear test were overlapped again and put at 130 °C for 3 h with 3 kPa constant pressure to ensure a

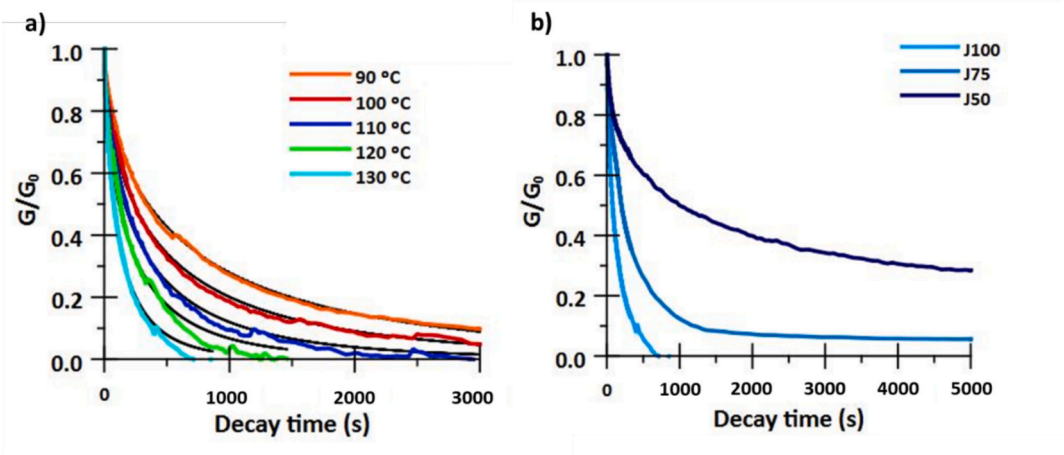

Fig. 4. a) Normalized stress relaxation curves at different temperatures for J100 material (colored) and their fitting curves using the KWW model (black). b) Comparison of the normalized stress relaxation curves at 130 °C of all three polyimines vitrimers.

Table 4
Stretching decay parameters, activation energy and adjusting parameters of the corresponding Arrhenius equation for all the materials prepared.

Sample	τ^{*} [a] (s)	β [b]	E_a (kJ/mol)	ln *A* (s)	r^2
J100	123	0.62	50 ± 8	−10 ± 2	0.99
J75	348	0.78	53 ± 28	−10 ± 5	0.96
J50	2460	0.44	101 ± 34	−22 ± 10	0.97

[a] Characteristic relaxation time at 130 °C using the KWW model.
[b] Average of β parameter for the different temperatures.

good contact between plates. It is worth noting that no additional initial formulation was added, which suggests that the re-adhesion will only be possible thanks to the bond-exchange reactions in the interface of the two layers. Fig. 5 shows the lap-shear test of the re-bonded adhesives, and Table 5 presents the data obtained. As it can be observed, excellent values of adhesive strength for the re-bonded polyimines could be obtained since, in all cases, they represent more than 75 % of the original value despite the fact that after failure, the re-adhesion may present some challenges caused by changes in the surface or in the adhesive such as roughening or a not perfect overlapping. In fact, J100 showed outstanding re-adhesion properties since almost the same adhesive strength could be achieved (97 %). Again, the higher flexibility of Jeff T403 makes the imine metathesis more likely to occur, which results in a higher amount of bond-exchange reactions taking place in the interface of both plates and therefore, better adhesion values are obtained.

3.6. *Mechanical recycling*

To analyze the mechanical recyclability, the three materials were ground into powder and hot pressed at 130 °C for 2 h under 3 MPa of pressure. This temperature was selected to ensure rapid dynamic behavior while at the same time maintaining structural integrity. As seen in Fig. S11, it was possible to mechanically reprocess the materials up to three times. To evaluate the properties of the recycled materials, DSC and DMTA analyses were performed (Fig. S12-S15), which revealed that no significant differences could be observed either in the T_g or in the thermomechanical properties, suggesting a successful mechanical recycling. Unfortunately, J50 became extremely brittle after the second mechanical recycling, being impossible to test under the same conditions as the others.

To compare the mechanical behavior of the virgin and recycled samples, the third recycled sample of J100 and J75 and the first recycled

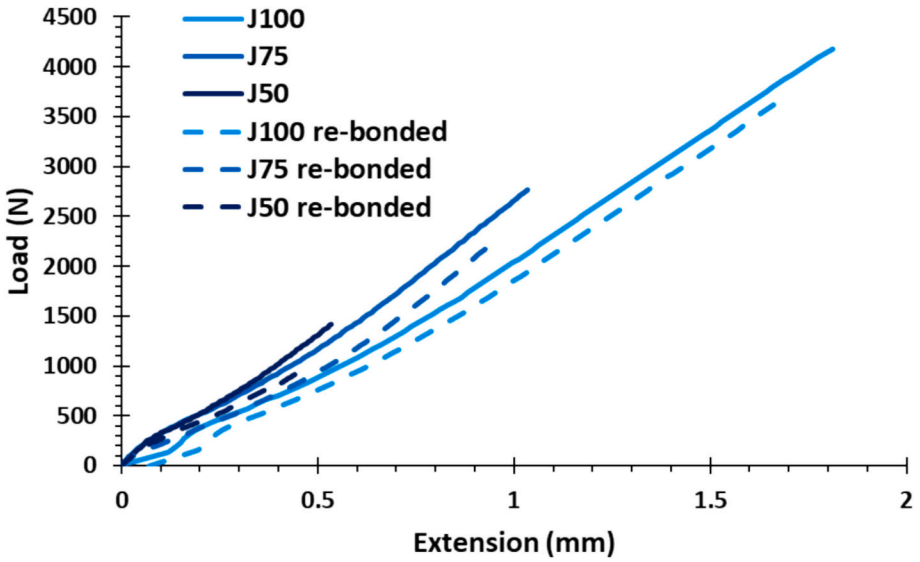

Fig. 5. Lap-shear curves of the virgin adhesives (solid lines) and of the re-bonded adhesives (dashed lines).

Table 5
Data from lap-shear tests of the virgin and re-bonded adhesives. The percentage with respect to the original lap-shear strength is indicated in parenthesis.

Sample	Virgin adhesives		*Re*-bonded adhesives	
	F_{max} [a] (N)	σ_{max} [b] (MPa)	F_{max} [a] (N)	σ_{max} [b] (MPa)
J100	3868 ± 230	12.4 ± 0.7	3652 ± 270 (97 %)	11.4 ± 1.1 (92 %)
J75	2158 ± 545	5.5 ± 3.0	2104 ± 821 (88 %)	5.0 ± 2.6 (91 %)
J50	1179 ± 213	3.8 ± 0.7	887 ± 243 (80 %)	2.8 ± 0.8 (75 %)

[a] Force at break.
[b] Stress at break.

on of J50 were tested in tensile and the main parameters were extracted. As can be seen in Fig. S16 the tensile stress-strain curves follow a similar trend to their counterparts. As seen in Table S2, the strength of all three materials is more or less similar although a slight increase in rigidity and fragility is detected due to the recycling process.

3.7. Chemical degradation

Imine bonds are known to hydrolyze under mildly acidic conditions, yielding both initial aldehyde (or ketone) and amine. Thus, J100 was used to investigate the degradation of the polymer and the possible recovery of the initial dialdehyde. After a mild acid treatment of 1 M HCl/THF (1:8 *v*/v) for 1 h, the solution turned brownish transparent, indicating that the polyimine was completely degraded (Fig. 6a). Then, after a simple work-up, a yellowish viscous liquid was obtained and analyzed by FTIR (Fig. S17) and NMR (Fig. S18 and S19). These results confirmed that the initial dialdehyde could be mainly recovered. However, the ^{1}H NMR also revealed some small signals corresponding to the initial vanillin which can be ascribed to the possible hydrolysis of some ester groups in those acid conditions.

Another approach to perform the degradation of the polyimines can be through mono- or di-amines that can undergo a transamination reaction, breaking down the polymer into smaller soluble imine molecules [28,39]. Thus, ethylenediamine and n-butylamine were used as reactive solvents to degrade the polymer. This method also proved to be adequate for degrading and solubilizing the final polymers (Fig. 6b and c) since after the whole treatment, a dark viscous liquid was obtained which was then analyzed by FTIR (Fig. S20). The FTIR spectrum revealed the complete disappearance of the ester groups of the material, possibly turning into an amide trough an amidation reaction. Therefore, this methodology proved to be even more effective than the acid hydrolysis in degrading the polyimines but useless in recovering the initial monomer due to side reactions during transamination.

As previously mentioned, one of the main problems of structural adhesives is the recovery of the adherents after the end of their lifetime. Therefore, both chemical degradation methodologies were used to degrade the adhesive after the failure. After treating the aluminum plates used in lap-shear tests with both methodologies, no polymer residues could be observed by the naked eye (Fig. S21). Moreover, the use of a digital microscope also confirmed the elimination of the adhesives from the surface of aluminum plates, confirming the degradation and the recovery of the initial adherents and highlighting that these materials can combine good adhesive properties but at the same time solve one of the main challenges of structural adhesives.

The resistance with other solvents that are nor acid media or amines was also performed in order to test their chemical stability. For this reason, solvents with different polarities namely, H_2O, ethyl acetate (EtOAc) and toluene (Tol) were selected. A piece of sample of each material remained immersed in each of the solvent for 24 h at room temperature. As can be appreciate in Fig. S22 after that time no changes can be seen indicating no chemical degradability.

3.8. Self-welding and repairability properties

As a proof of concept, the self-welding ability of the J100 was tested due to its excellent and fast dynamic properties. To do that, a rectangular sample of J100 was die cut with a circular punch of 6 mm diameter and repaired using a circular patch with a slightly higher diameter to ensure a perfect surface contact (8 mm) crafted from identical material (see Fig. S23).

Next, the material was heated at 130 °C for 3 h under a slight pressure of 1 MPa to ensure optimal contact between the two parts and to

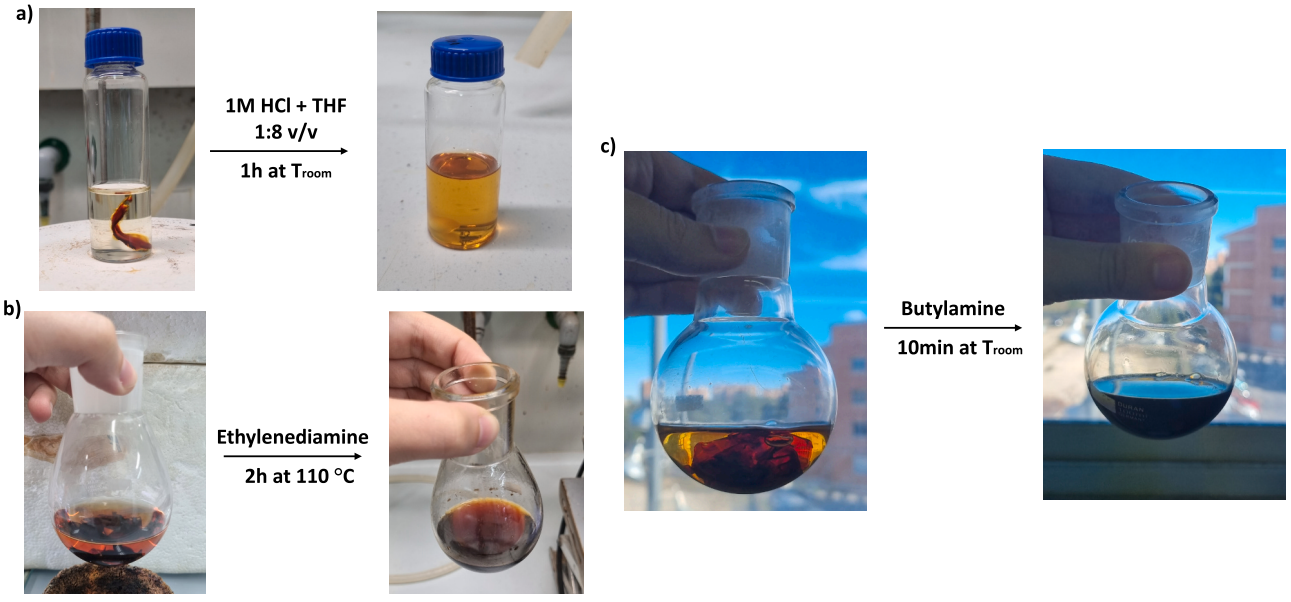

Fig. 6. Photographs of the chemical degradation of J100 using a) acidic conditions, b) ethylenediamine, and c) n-butylamine.

Table 6
Comparison of engineering stress and strain at break and tensile modulus of original, repaired and holed samples of J100 material. The efficiency of the repaired process in comparison to the virgin one is also included in brackets.

Sample	σ_b[a] (MPa)	ε_b[b] (%)	E_T[c] (MPa)
J100	22 ± 1	208 ± 25	399 ± 10
Repaired	24 ± 5 (109 %)	166 ± 3 (80 %)	456 ± 18 (114 %)
Holed	16 ± 2	1.7 ± 2	930 ± 47

[a] Stress at break.
[b] Strain at break.
[c] Tensile modulus.

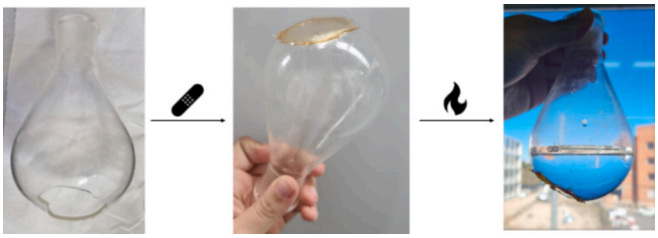

Fig. 7. Reparation of a broken flask with J100.

facilitate the imine exchange process. Subsequently, tensile stress-strain tests were conducted on the original, the holed (without repairing) and the repaired sample. As presented in Fig. S24 and Table 6, the holed sample could not achieve the original stress and strain levels and broke earlier than the original sample, as expected due to the stress concentration phenomenon. In contrast, the repaired sample presented stress values similar to the original, albeit without reaching the same degree of deformation and presenting slightly lower values. Notably, none of the repaired samples experienced failure at its repaired section and rather, they broke underneath, indicating that the repaired area was not the weakest point and that the stress concentration phenomenon was eliminated (See Fig. S25).

To showcase the excellent repair capabilities of polyimines, a pre-cured J100 vitrimer was die-cut into the shape of a fractured pear flask and subsequently cured. As presented in Fig. 7, the mended flask could successfully retain water without any leaks, highlighting the versatility of the material for repairing glass, aluminum, or even self-repairing its own damage.

4. Conclusions

A series of vanillin-based polyimine vitrimers were successfully prepared from a synthesized dialdehyde (GV) and the subsequent curing with different proportions of two amines (Jeff T403 and mXDA). All the materials showed T_gs ranging from 20 to 60 °C, good thermal stability ($T_{2\%}$ > 210 °C), and tunable mechanical properties at service temperatures depending on their network architecture.

The materials showed excellent and rapid dynamic behavior through the well-known imine metathesis, even at relatively low temperatures and without the addition of an external catalyst (5 min at 160 °C).

Additionally, thanks to a pre-cured state, gelled and malleable adhesives could be prepared and adapted to complex surfaces to create complex adhesive joints. Similar or even better adhesive strength than previously reported similar CANs (> 12 MPa for J100) were obtained in all cases. Moreover, the excellent vitrimeric properties of these polyimines enabled the re-bonding of the aluminum plates after failure, without adding extra initial formulation, reaching up to 97 % of original adhesive strength, thus demonstrating a successful re-adhesion.

Besides, the polyimines could not only be mechanically recycled up to three times without significant differences in their T_g values and their thermomechanical properties, but also chemically degraded via acid hydrolysis or via transamination. The former method allowed to recover the original monomer. Additionally, this chemical degradability enabled the recovery of the original adherents after the adhesion, representing a significant advancement in addressing one of the main challenges of structural adhesives. Finally, these polyimine materials exhibited remarkable self-welding capabilities, and excellent repairability, significantly enhancing their potential for advanced applications in the industrial sector.

CRediT authorship contribution statement

Anna Vilanova-Pérez: Writing – original draft, Methodology, Investigation, Formal analysis, Data curation. **Marc Surós:** Formal analysis, Data curation. **Àngels Serra:** Writing – review & editing, Validation, Funding acquisition, Conceptualization. **Silvia De la Flor:** Writing – review & editing, Validation, Supervision, Funding acquisition, Conceptualization. **Adrià Roig:** Writing – review & editing, Visualization, Validation, Supervision, Conceptualization.

Declaration of competing interest

The authors declare no competing financial interest or personal relationships that could have appeared to influence the work reported in this paper.

Data availability

Data will be made available on request.

Acknowledgments

This work is part of the R&D projects PID2020-115102RB-C21 and TED2021-131102B-C22 funded by MICIU/AEI/10.13039/501100011033 and FEDER/UE and European Union "NextGenerationEU"/PRTR. We acknowledge these grants, and we also thank to the Generalitat de Catalunya (2021-SGR-00154).

Appendix A. Supplementary data

Supplementary data to this article can be found online at https://doi.org/10.1016/j.reactfunctpolym.2024.106109.

References

[1] S. Ebnesajjad, Characteristics of adhesive materials, in: Handbook of Adhesives and Surface Preparation, William Andrew Publishing, 2011, pp. 137–183, https://doi.org/10.1016/B978-1-4377-4461-3.10008-2.
[2] M.Q. dos Reis, M.D. Banea, L.F.M. da Silva, R.J.C. Carbas, Mechanical characterization of a modern epoxy adhesive for automative industry multi-material adhesive joints for automotive industry, J. Braz. Soc. Mech. Sci. Eng. 41 (2019) 1–11, https://doi.org/10.1007/s40430-019-1844-2.
[3] M.D. Banea, M. Rosioara, R.J.C. Carbas, L.F.M. da Silva, Multi-material adhesive joints for automotive industry, Comp. Part B. 151 (2018) 71–77, https://doi.org/10.1016/j.compositesb.2018.06.009.
[4] Y. Ma, Z. Kou, Y. Hu, J. Zhou, Y. Bei, L. Hu, Q. Huang, P. Jia, Y. Zhou, Research advances in bio-based adhesives, Int. J. Adhes. Adhes. 126 (2023) 103444–103461, https://doi.org/10.1016/j.ijadhadh.2023.103444.
[5] F. Awaja, M. Gilbert, G. Kelly, B. Fox, P.J. Pigram, Adhesion of polymers, Prog. Polym. Sci. 34 (2009) 948–968, https://doi.org/10.1016/j.progpolymsci.2009.04.007.
[6] A. Hutchinson, Y. Liu, Y. Lu, Overview of disbanding technologies for adhesive bonded joints, J. Adhes. 93 (2017) 737–755, https://doi.org/10.1080/00218464.2016.1237876.
[7] C.J. Kloxin, C.N. Bowman, Covalent adaptable networks: smart, reconfigurable and responsive network systems, Chem. Soc. Rev. 42 (2013) 7161–7173, https://doi.org/10.1039/C3CS60046G.
[8] J. Zheng, Z.M. Png, S.H. Ng, G.X. Tham, E. Ye, S.S. Goh, X.J. Loh, Z. Li, Vitrimers: current research trends and their emerging applications, Mater. Today 51 (2021) 586–625, https://doi.org/10.1016/j.mattod.2021.07.003.
[9] D. Santiago, D. Guzmán, J. Padilla, P. Verdugo, S. De la Flor, À. Serra, Recyclable and reprocessable epoxy vitrimer adhesives, ACS Appl. Polym. Mater. 5 (2023) 2006–2015, https://doi.org/10.1021/acsapm.2c02063.

[10] V.R. Madduluri, A. Bendi, G.P. Chinmay, R. Maniam, M.H.A. Roslan, Rahim, Recent advances in vitrimers: a detailed study on the synthesis, properties and applications of bio-vitrimers, J. Polym. Environ. (2024), https://doi.org/10.1007/s10924-024-03416-0.
[11] X. Fan, J. Zheng, J.C.C. Yeo, S. Wang, K. Li, J.K. Muiruri, N. Hadjichristidis, Z. Li, Dynamic covalent bonds enabled carbon fiber reinforced polymers recyclability and material circularity, Angew. Chem. Int. Ed. 63 (2024) 1–25, https://doi.org/10.1002/anie.202408969.
[12] N.J. Van Zee, R. Nicolaÿ, Vitrimers: permanently crosslinked polymers with dynamic network topology, Prog. Polym. Sci. 104 (2020) 101233, https://doi.org/10.1016/j.progpolymsci.2020.101233.
[13] M. Guerre, C. Taplan, J.M. Winne, F.E. Du Prez, Vitrimers: directing chemical reactivity to control material properties, Chem. Sci. 11 (2020) 4855–4870, https://doi.org/10.1039/D0SC01069C.
[14] A. Duval, W. Benali, L. Avérous, Turning lignin into a recyclable bioresource transesterification vitrimers from lignins modified with ethylene carbonate, Green Chem. 26 (2024) 8414–8428, https://doi.org/10.1039/d4gc00567h.
[15] E. Rossegger, R. Höller, D. Reisinger, J. Strasser, M. Fleisch, T. Griesser, S. Schlögl, Digital light processing 3D printing with thiol-acrylate vitrimers, Polym. Chem. 12 (2021) 639–644, https://doi.org/10.1039/D0PY01520B.
[16] G. Ye, S. Huo, C. Wang, Q. Zhang, H. Wang, P. Song, Z. Liu, Strong yet tough catalyst-free transesterification vitrimer with excellent fire-retardancy, durability, and closed-loop recyclability, Small (2024) 2404634–2404644, https://doi.org/10.1002/smll.202404634.
[17] Z. Liu, Y. Tang, Y. Chen, Z. Lu, Z. Riu, Dynamic covalent adhesives and their applications: current progress and future perspectives, Chem. Eng. J. 497 (2024) 154710–154732, https://doi.org/10.1016/j.cej.2024.154710.
[18] A. Roig, V. D'Agostino, À. Serra, S. De la Flor, Towards fast relaxation rates and creep resistance in disulfide vitrimer-like materials, React. Funct. Polym. 193 (2023) 105764, https://doi.org/10.1016/j.reactfunctpolym.2023.105764.
[19] P. Verdugo, D. Santiago, S. De la Flor, À. Serra, A biobased epoxy vitrimers with dual relaxation mechanism: a promising material for renewable, reusable and recyclable adhesives and composites, ACS Sustain. Chem. Eng. 12 (2024) 5965–5978, https://doi.org/10.1021/acssuschemeng.4c00205.
[20] J. Liu, A. Pich, K.V. Bernaerts, Preparation of lignin-based vinylogous urethane vitrimer materials and their potential use as on-demand removable adhesives, Green Chem. 26 (2024) 1414–1429, https://doi.org/10.1039/d3gc02799f.
[21] R. Yang, W. Li, R. Mo, X. Zhang, Recyclable biobased dynamic cross-linking epoxy thermosets containing vinylogous urethane bonds with shape memory properties, ACS Appl. Polym. Mater. 5 (2023) 9395–9402, https://doi.org/10.1021/acsapm.3c01879.
[22] A. Roig, L. Molina, À. Serra, D. Santiago, S. De la Flor, Structural reversible adhesives based on thiol-epoxy vitrimers, Polym. Test. 128 (2023) 108205–108214, https://doi.org/10.1016/j.polymertesting.2023.108205.
[23] Z. Zhou, X. Su, J. Liu, R. Liu, Synthesis of vanillin-based polyimine vitrimers with excellent reprocessability, fast chemical degradability, and adhesion, ACS. Appl. Polym. Mater. 2 (2020) 5716–5725, https://doi.org/10.1021/acsapm.0c01008.
[24] F. Van Lijsebetten, T. Maiheu, J.M. Winne, F.E. Du Prez, Epoxy adhesives with reversible hardeners: controllable thermal debonding in bulk and at interfaces, Adv. Mater. 35 (2023) 2300802, https://doi.org/10.1002/adma.202300802.
[25] M.E. Belowich, J.F. Stoddart, Dynamic imine chemistry, Chem. Soc. Rev. 41 (2021) 2003–2024, https://doi.org/10.1039/c2cs15305j.
[26] N. Fanjul-Mosteirín, K. Odelius, Covalent adaptable networks with tailorable material properties based on divanillin polyimines, Biomacromolecules 25 (2024) 2348–2357, https://doi.org/10.1021/acs.biomac.3c01224.
[27] R. Dinu, A. Pidvorotnia, D.D. Swanson, A. Mija, Bio-derived epoxy thermosets incorporating imine linkages: towards sustainable and advanced polymer materials, Chem. Eng. J. 499 (2024) 156486–156501, https://doi.org/10.1016/j.cej.2024.156486.
[28] Y. Qu, X. Lu, Z. Xin, Biobased polybenzoxazone vitrimer with imine bonds: shape memory, reprocessing, and degradation, ACS Sustain. Chem. Eng. 12 (2024) 7739–7747, https://doi.org/10.1021/acssuschemeng.4c00052.
[29] M.A. Rashid, S. Zhu, L. Zhang, K. Jin, W. Liu, High-performance and fully recyclable epoxy resins cured by imine-containing hardeners derived from vanillin and syringaldehyde, Eur. Polym. J. 187 (2023) 111878, https://doi.org/10.1016/j.eurpolymj.2023.111878.
[30] M.A. Lucherelli, A. Duval, L. Averous, Combining associative and dissociative dynamic linkages in covalent adaptable networks from biobased 2,5-furandicarboxaldehyde, ACS Sustain. Chem. Eng. 11 (2023) 2334–2344, https://doi.org/10.1021/acssuschemeng.2c05956.
[31] P. Li, J. Zhang, J. Ma, C. Xu, X. Liang, T. Yuan, Y. Hu, Z. Yang, Fully bio-based thermosetting polyimine vitrimers with excellent adhesion, rapid self-healing, multi-recyclability and antibacterial ability, Ind. Crop. Prod. 204 (2023) 117288–117298, https://doi.org/10.1016/j.indcrop.2023.117288.
[32] K.S. Fancey, A mechanical model for creep, recovery and stress relaxation in polymeric materials, J. Mater. Sci. 40 (2005) 4827–4831, https://doi.org/10.1007/s10853-005-2020-x.
[33] L. Li, X. Chen, K. Jin, J.M. Torkelson, Vitrimers designed both to strongly suppress creep and to recover original cross-link density after reprocessing: quantitative theory and experiments, Macromolecules 51 (2018) 5537–5546, https://doi.org/10.1021/acs.macromol.8b00922.
[34] A. Dhinojwala, J.C. Hooker, J.M. Torkelson, Retardation of rotational reorientation dynamics in polymers near the glass transition: a novel study over eleven decades in time using second-order non-linear optics, J. Non-Cryst. Solids 172-174 (1994) 286–296, https://doi.org/10.1016/0022-3093(94)90447-2.
[35] ASTM, D638–14, Standard test method for tensile properties of plastics, 2014.
[36] UNE-EN ISO 1465, Adhesives. Determination of tensile lap-shear strength of bonded assemblies, 2009.
[37] UNE-EN ISO 13887, Structural adhesives. Guideline for Surface preparation of metals and plastics prior to adhesive bonding, 2004.
[38] C. Russo, F. Bustamante, X. Fernández-Francos, S. De la Flor, Adhesive properties of thiol-acrylate-epoxy composites obtained by dual-curing procedures, Int. J. Adhes. Adhes. 112 (2022) 102959, https://doi.org/10.1016/j.ijadhadh.2021.102959.
[39] H. Memon, Y. Wei, L. Zhang, Q. Jiang, W. Liu, An imine-containing epoxy vitrimer with versatile recyclability and its application in full recyclable carbon fiber reinforced composites, Compos. Sci. Technol. 199 (2020) 108314–108325, https://doi.org/10.1016/j.compscitech.2020.108314.